Available online at www.sciencedirect.com
ScienceDirect
Biochimica et Biophysica Acta 1768 (2007) 207–217
Biochimica et Biophysica Acta BBA
www.elsevier.com/locate/bbamem

Vitamin B_1 thiazole derivative reduces transmembrane current through ionic channels formed by toxins from black widow spider venom and sea anemone in planar phospholipid membranes

Oleg Ya. Shatursky [a,*], Tatyana M. Volkova [b,†], Olexander V. Romanenko [c], Nina H. Himmelreich [a], Eugene V. Grishin [b]

[a] *Department of Neurochemistry, Palladin Institute of Biochemistry, Leontovich Str., 9, 01601, Kiev, Ukraine*
[b] *Shemiakin and Ovchinnikov Institute of Bioorganic Chemistry, Miklukho-Maklai Str., 16/10, 117871, Moscow, Russian Federation*
[c] *Department of Biology, Bogomolets National Medical University, Pobedy av., 34, 03680, Kiev, Ukraine*

Received 9 February 2006; received in revised form 21 October 2006; accepted 26 October 2006
Available online 1 November 2006

Abstract

The vitamin B_1 (thiamine) structural analogue 3-decyloxycarbonylmethyl-4-methyl-5-(β-hydroxyethyl) thiazole chloride (DMHT) (0.1 mM) reversibly reduced transmembrane currents in $CaCl_2$ and KCl solutions via ionic channels produced by latrotoxins (α-latrotoxin (α-LT) and α-latroinsectotoxin (α-LIT)) from black widow spider venom and sea anemone toxin (RTX) in the bilayer lipid membranes (BLMs). Introduction of DMHT from the cis-side of BLM bathed in 10 mM $CaCl_2$ inhibited transmembrane current by 31.6±3% and by 61.8±3% from the trans-side of BLM for α-LT channels. Application of DMHT in the solution of 10 mM $CaCl_2$ to the cis-side of BLM decreased the current through the α-LIT and RTX channels by 52±4% and 50±5%, respectively. Addition of Cd^{2+} (1 mM) to the cis- or trans-side of the membrane after the DMHT-induced depression of Ca^{2+}-current across the α-LT channels caused its further decrease by 85±5% that coincides favorably with the intensity of Cd^{2+} blocking in control experiments without DMHT. These data suggest that DMHT inhibiting is not specific for latrotoxin channels only and DMHT may exert its action on α-LT channels without considerable influence on the ionogenic groups of Ca^{2+}-selective site inside the channel cavity. The binding kinetics of DMHT with the α-LT channel shows no cooperativity and allows to expect that the DMHT binding site of the toxin is formed by one ionogenic group as the slopes of inhibition rate determined in log–log coordinates are 1.25 on the trans-side and 0.68 on the cis-side. Similar pK of binding (5.4 on the trans-side and 5.7 on the cis-side) also suggest that DMHT may interact with the same high affinity site of α-LT channel on either side of the BLM. The comparative analysis of effective radii measured for α-LT, α-LIT and RTX channels on the cis-side (0.9 nm, 0.53 nm and 0.55 nm, correspondingly) and for α-LT channel on the trans-side (0.28±0.18 nm) with the intensity of DMHT inhibitory action obtained on these channels allowed to conclude that the potency of DMHT inhibition increased on toxin pores of smaller lumen.

Keywords: Lipid bilayer; α-latrotoxin; α-latroinsectotoxin; Sea anemone toxin; Ion channel; Vitamin B_1; Thiazole analogue

1. Introduction

Vitamin B_1 thiazole derivatives were shown to depress spontaneous and evoked quantum transmitter release in cholinergic synapses of vertebrate skeletal muscles [1,2,3]. Application of DMHT, known as the most effective vitamin B_1 structural analogue, completely eliminated neuromediator release induced by α-LT [1,2]. However, the molecular pharmacology mechanism for the interaction of thiamine thiazole derivatives with excitable membrane remains unclear. It was suggested that the thiazole moiety of their molecules may bind to thiamine-sensitive membrane structures [1,2]. It is also possible that the DMHT-induced block of α-LT presynaptic action was a result of its direct interaction with α-LT channels formed in the excitable membrane of vertebrates [4].

α-LIT is another pore-forming neurotoxin that belongs to the family of latrotoxins [5,6] and, unlike α-LT, binds exclusively

* Corresponding author. Fax: +044 279 63 65.
E-mail address: olegshatursky@biochem.kiev.ua (O.Y. Shatursky).
† Deceased.

0005-2736/$ - see front matter © 2006 Elsevier B.V. All rights reserved.
doi:10.1016/j.bbamem.2006.10.012

with the nerve tissue of invertebrates [5]. α-LIT has also an ability to induce the increase in frequency of miniature excitatory postsynaptic potentials at the insect neuromuscular junction [5]. It is likely that despite some structural divergence that causes a tissue specificity and affects the channel properties, the main structure and physiological action of α-LIT is still very similar to α-LT [6,7,8,9,10,11]. Therefore, DMHT was also expected to interact with α-LIT channels in a bilayer membrane. Unrelated RTX channels [12,13] were used to determine the specificity of DMHT to the latrotoxins. The data presented below demonstrate that DMHT inhibits Ca^{2+} and K^{+} currents through the ion channels formed by α-LT, α-LIT and RTX in a bilayer lipid membrane. A preliminary report of this work has been presented in [14].

2. Materials and methods

2.1. Protein isolation

α-LT and α-LIT were isolated from *Latrodectus mactans tradecimgutatus* crude venom or venom glands by fractionation on a MONO Q column (Pharmacia, Sweden) described in [5,15]. RTX from sea anemone *Radianthus macrodactylus* was purified and tested by Dr. M.M. Monastirnaya at Pacific Ocean Institute of Bioorganic Chemistry (Vladivostok, Russian Federation) as described in [12,13].

2.2. Bilayer membranes formation

Planar membranes were formed from a solution of phosphatidylcholine (PC) (Kharkov factory of biopreparations Biolek, Ukraine, Sigma, USA) and cholesterol (Calbiochem, Germany, Sigma, USA) in n-heptane applied onto a 0.6 mm hole in a Teflon cup held within a glass chamber. The PC and cholesterol were maintained at a ratio of 50.2 mol% PC and 49.8 mol% cholesterol. The total lipid concentration in heptane solution was 20 mg/ml. The formation of bilayer membrane was visually monitored with an MBC-9 binocular microscope (St. Petersburg Optico-Mechanical Plant LOMO, Russian Federation). The internal volume of the Teflon cup was 1 ml, whilst the outer compartment contained 9 ml of the bathing solution. The membrane separated solution contained 10 mM Tris–HCl (pH 7.4) (Sigma, USA) and the required quantities of analytical grade calcium chloride (Sigma, USA), potassium chloride and cadmium chloride (Donetsk factory of Chemical Reagents Reachim, Ukraine).

The buffer solutions in both chambers could be stirred as required.

2.3. Voltage-clamping experiments

Voltage was controlled and voltage-clamp recordings of membrane current were made via a high resolution home made amplifier with 1 kHz bandwidth. The Teflon cup was referred to as the trans-side of the membrane, which was defined as zero. The outer glass chamber was referred to as the cis-side. The cis- and trans-chambers were connected to the amplifier by silver chloride electrodes immersed in a 2 M KCl solution with 0.2 M KCl agar bridges. The polarization potential between the electrodes did not exceed 1.5 mV. Voltage-ramp protocols of 100 mV/1 min or holding potentials between − 100 mV and 100 mV were applied by the voltage source. Membrane currents were recorded on an N307/1 XY recorder (Krasnodar Plant of Measuring Instruments, ZIP, Russian Federation). Semi-conductor thermobatteries TEMO-3 (Lvov Factory Electronpribormash, Ukraine) were used to apply a temperature ramp. Continuos stirring of the bathing solutions minimized the error due to uneven warming or cooling. Activation energy of ion transport through α-LT modified BLM was defined as in [6].

Tetrabutylammonium chloride (TBA) (Aldrich, Germany) was used in the conductance blocking experiments as one of tetraalkylammoniums to traverse the 1.1 nm diameter toxin pore [16]. Thiazole derivative of thiamin 3-decyloxycarbonylmethyl-4-methyl-5-(2-hydroxyethyl) thiazole chloride (DMHT):

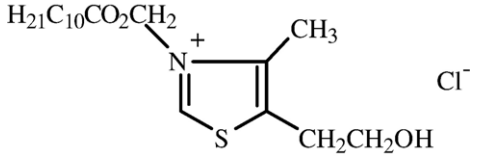

applied to all the toxin channels in lipid bilayers was synthesized by Dr. A.I. Vovk at the Institute of Bioorganic Chemistry and Petroleum Chemistry (Kiev, Ukraine) as described in [3].

2.4. Determination of α-LT and α-LIT pore size

The radii of the pores formed by toxins were defined by the method of Krasilnikov et al. [17]. Low-molecular-weight nonelectrolytes (NEs) of analytical grade, including ethylene glycol (Shostka Factory of Chemical Reagents Reachim, Ukraine, Riedel-de Haen, Germany) glycerol (Shostka Factory of Chemical Reagents Reachim, Ukraine, Sigma-Aldrich, USA) glucose (Shostka Factory of Chemical Reagents Reachim, Ukraine, Fluka, France), sucrose (Shostka Factory of Chemical Reagents Reachim, Ukraine, Fluka, Germany) and polyethylene glycols (PEGs) with average molecular weights of 300, 400, 600, 1000, 1500, 2000, 3000, 4000, 6000 and 2000) (Fluka, Switzerland, Sigma-Aldrich, USA), were mixed with a 100 mM solution of KCl in 10 mM Tris–HCl (pH 7.4) to be used as membrane-bathing fluids at a final concentration of 20%.

All experiments were carried out at a room temperature (20 to 24 °C) unless stated otherwise. Hereinafter, mean values±standard errors are indicated for 8–10 experiments, each one made on a separately painted BLM.

3. Results

3.1. Incorporation of α-LT, α-LIT and RTX channels into BLM

The introduction of α-LT, α-LIT or RTX (data not shown) into the chamber with a membrane in bathing solutions of 10 mM $CaCl_2$ or 100 mM KCl caused a step like increase in current readily (Figs. 1a, 2a, 3A, inset a). Estimates of the discrete channel conductances in 100 mM KCl solution at + 60 mV obtained on more than 100 separate events suggested a peak of maximal conductance on amplitude histogram at 165 pS for relatively large α-LT channels (further referred as the most probable conductance of single α-LT channel) (Fig. 1a). The α-LIT channel conductance was much smaller and, therefore, a single channel conductance was determined as the mean value± standard deviations of all the conductances represented on the histogram. Thus defined, unitary α-LIT channel conductance was 23.5±4.8 pS (Fig. 2a, Table 1). The current–voltage (I/V) relationships and temperature dependence were determined as membrane conductance reached a steady-state level.

3.2. Ion-conductive properties of α-LT channels after DMHT-induced inhibition

Introduction of DMHT (0.1 mM) to the *cis*-compartment containing 10 mM $CaCl_2$ membrane washing solution inhibited the current through α-LT channels by 31.6±3%. Addition of DMHT to the trans-side resulted in a 61.8±3% decrease in α-LT-induced current. The DMHT-induced inhibition of trans-membrane current occurred within 3 to 5 min after addition of DMHT and did not exhibit significant dependence on the sign of

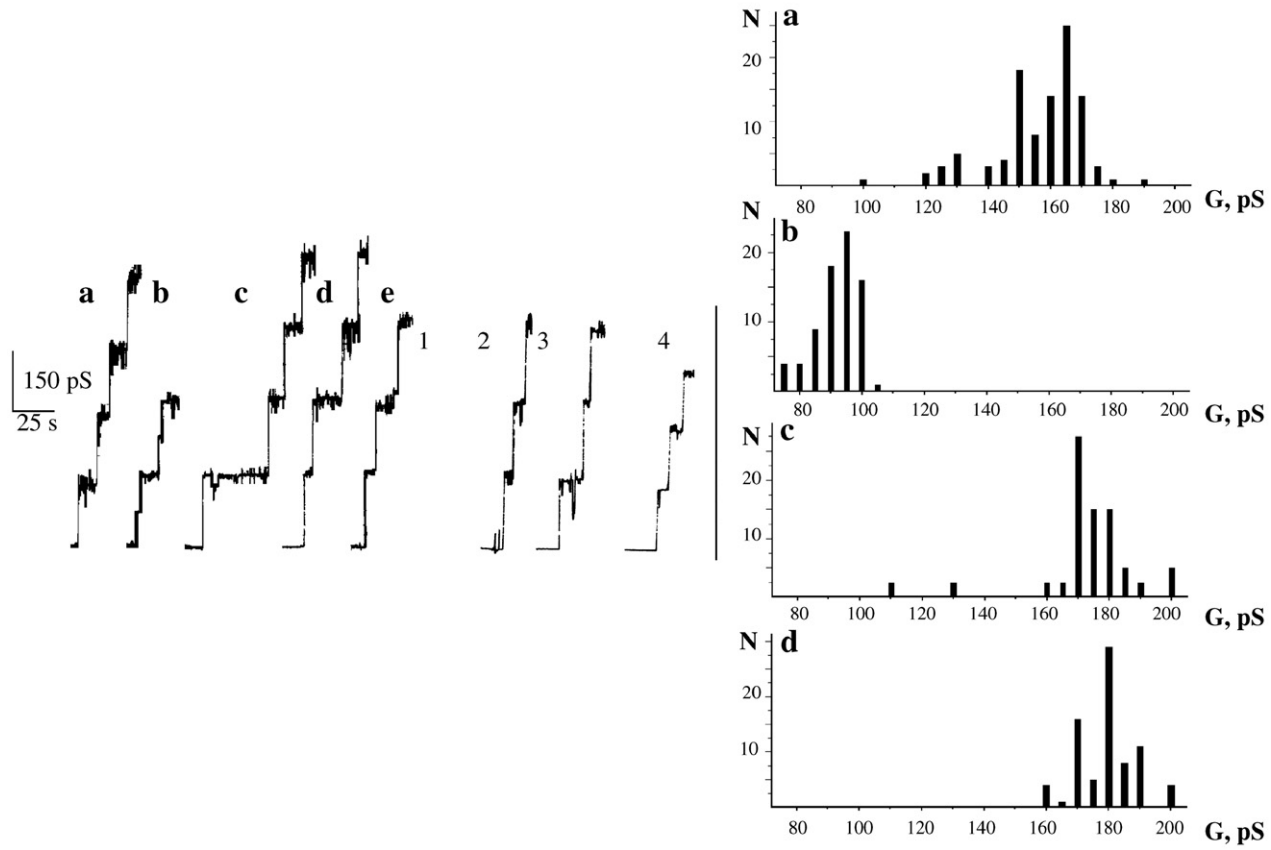

Fig. 1. Amplitude histogram of α-LT single channel conductance in a voltage-clamped bilayer membrane at +60 mV. Basic membrane separated solution contained: (a) 100 mM KCl and 10 mM Tris–HCl (pH 7.4); (b) basic solution with 20% ethylene glycol, (c) 20% PEG 1000, (d) 20% PEG 6000 added on both sides of the membrane and (e) with 1, 20% sucrose from the trans-side; 2, 20% glucose from the trans-side; 3, 20% glycerol from the trans-side; 4, 20% ethylene glycol from the trans-side and 20% PEG 1000 from the cis-side of the membrane. α-LT single channel recordings under corresponding conditions are shown on the left. Channel openings are upward deflections. In all the experiments, toxin was introduced to the cis-side of the membrane. The final concentration of α-LT in the cis-chamber was 0.0126 ng/ml.

the membrane potential (Fig. 3A, B). Sequential additions of DMHT in control experiments on "channel-free" membranes decreased the membrane stability and led to its eventual rupture at concentrations of 3 to 5 mM. This suggests that the DMHT may partition into hydrophobic phase of the lipid bilayer.

3.2.1. The influence of cadmium ions on DMHT-induced inhibition of α-LT channels

The addition of $CdCl_2$ (1 mM) to the cis-compartment with DMHT (0.1 mM) after the DMHT-induced depression of transmembrane current across α-LT channel caused further decrease in Ca^{2+}-current by 85±5% in the symmetrical solution of 10 mM $CaCl_2$. Application of Cd^{2+} onto a α-LT-induced current from the trans-side of the BLM after the DMHT inhibition made from the same side also resulted in 85±5% block of Ca^{2+}-current. This coincides favorably with the intensity of Cd^{2+} blocking of Ca^{2+}-current via α-LT channels without DMHT (Fig. 3A, insets b and c). These data suggest no considerable influence of DMHT molecule on low-affinity Ca^{2+}-selective site found inside α-LT channel [18]. This is confirmed by the fact that perfusion of 10 mM $CaCl_2$ completely restored the initial α-LT conductance measured before the introduction of DMHT.

3.2.2. The effect of different concentrations of DMHT on α-LT channels

The DMHT inhibition of α-LT channels in 10 mM $CaCl_2$ solution was dependent upon the concentration of the inhibitor and could be described by a Langmuir saturation curve (Fig. 4). The reduction of α-LT channels conductance occurs steeply in an exponential manner with increasing DMHT concentration and reaches a saturation at 0.01 mM from either side of the membrane (Fig. 4, inset). The rate of inhibition was defined as the conductance change after addition of each DMHT concentration, which when plotted on double-log coordinates was linear. One half of maximum binding velocity was achieved at a DMHT concentration of 4 μM on the trans-side and 2 μM on the cis-side of the bilayer membrane. The DMHT binding constant determined in double-log coordinates was $10^{5.4}$ M^{-1} on the trans-side and $10^{5.7}$ M^{-1} on the cis-side with the slopes of 1.25 and 0.68, correspondingly.

3.2.3. The temperature dependence

The addition of DMHT to the cis-side of the membrane did not change significantly the activation energy (E_a) for Ca^{2+}-current through α-LT channels (8.501±0.879 kJ/mol in 10 mM

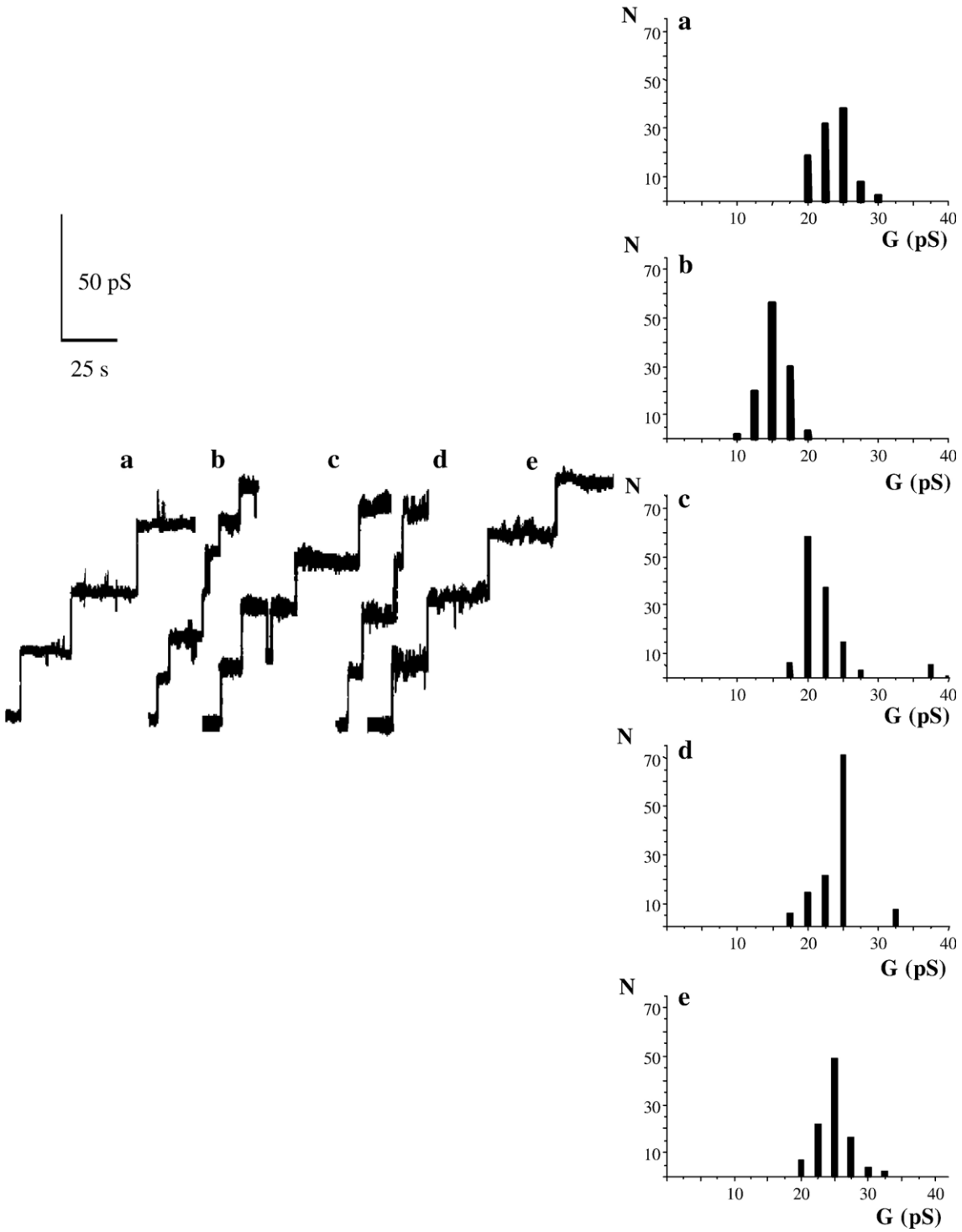

Fig. 2. Amplitude histogram of α-LIT unitary channel conductances at a membrane potential of +60 mV. Basic membrane bathing solution contained: (a) 100 mM KCl and 10 mM Tris–HCl (pH 7.4); (b) basic solution with 20% ethylene glycol, (c) 20% sucrose, (d) 20% PEG 300 and (e) PEG 6000 from both sides of the membrane. α-LIT single channel recordings under corresponding conditions are shown on the left. Channel openings are upward deflections. In all the experiments, α-LIT was added to the cis-chamber at a final concentration of 0.043 ng/ml.

$CaCl_2$ and 9.255±0.126 kJ/mol after the DMHT-induced inhibition was complete), while addition of Cd^{2+} (1 mM) increased the E_a (12.102±0.419 kJ/mol) (Fig. 5). These data indicate that Ca^{2+} must overcome a greater activation barrier to pass through the channel after the interaction of Cd^{2+} with the charged groups of α-LT.

3.2.4. The effect of ion substitution

Introduction of DMHT (0.1 mM) into the cis-compartment did not produce a significant change of transmembrane current through α-LT channels in the symmetrical solution of 100 mM KCl. Five minutes after addition, it inhibited the inward K^+-current by 11±3% (Fig. 6A, curve 2). Addition of DMHT

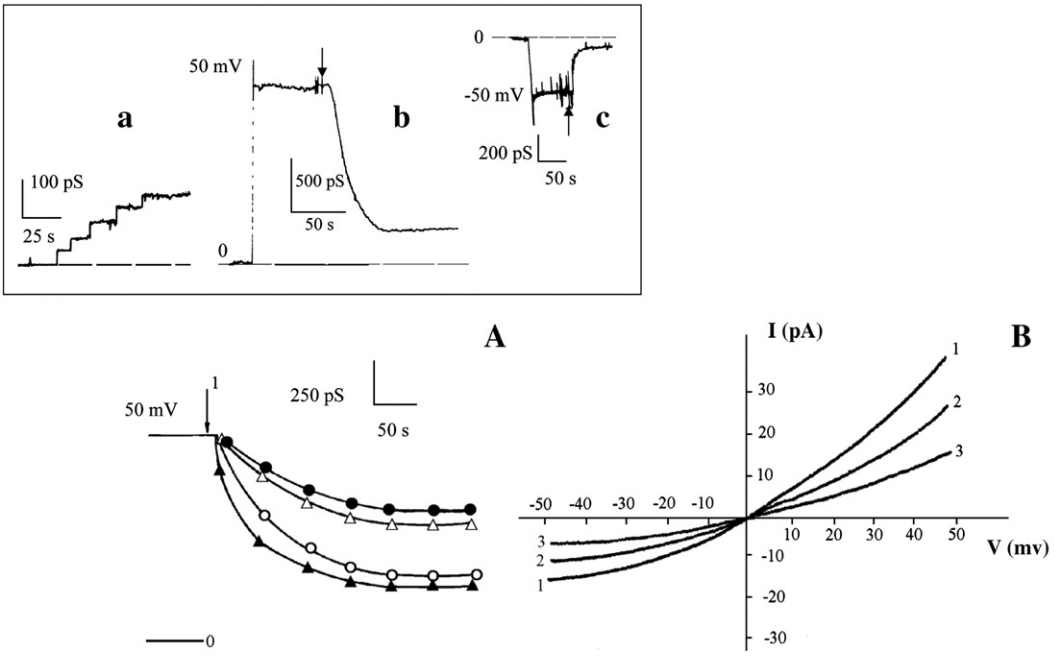

Fig. 3. Blocking of the steady-state Ca^{2+}-current through α-LT channels by DMHT (0.1 mM) and Cd^{2+} (1 mM). The membrane was bathed in a symmetric solution of 10 mM $CaCl_2$. (A) The time-courses of α-LT-induced current at different holding potentials after addition of DMHT to the cis-side of the membrane: (●)—+50 mV, (△)—−50 mV and to the trans-side of the membrane: (▲)—+50 mV, (○)—−50 mV. The arrow 1 indicates addition of DMHT. Each point represents the mean value of 8–10 experiments carried out on a separate membrane. Standard errors did not exceed the size of experimental points. The inset represents: (a) α-LT single channel recording made in a symmetric solution of 10 mM $CaCl_2$ at + 50 mV, (b) the time-trace of α-LT-induced current at +50 mV in a symmetric solution of 10 mM $CaCl_2$ after addition of $CdCl_2$ to the cis-side of membrane, (c) the time-trace of α-LT-induced current at −50 mV in symmetric solution of 10 mM $CaCl_2$ after addition of $CdCl_2$ to the trans-side of the BLM. The arrows indicate addition of Cd^{2+}. Dashed line shows zero current. (B) Current–voltage relationships of α-LT channels determined using the voltage ramp protocol (−50 mV to +50 mV, 1 min) in a symmetric solution of 10 mM $CaCl_2$ (plot 1), after the addition of DMHT to the cis-side of the membrane (plot 2) and to the trans-side of the membrane (plot 3). All experiments represented on the right panel were made on one membrane. Trans-application of DMHT was made after careful washout (80 ml) of cis-chamber with 10 mM $CaCl_2$. Separate addition of DMHT to the trans-side or the cis-side of the BLM without previous DMHT inhibiting and perfusion of 10 mM $CaCl_2$ from the opposite side of membrane produced the same inhibition of Ca^{2+}-current (data not shown). The α-LT was added to the cis-side of the membrane at a final concentration of 0.01 ng/ml.

(0.1 mM) to the trans-side of the BLM blocked two times more K^+-current (data not shown). In both cases the intensity of DMHT inhibitory action did not depend on the sign of membrane potential. Thus, despite obvious differences between DMHT-induced inhibition in 10 mM $CaCl_2$ (61.8±3% on the trans- and 31.6±3% on the cis-side) (Fig. 3) and 100 mM KCl solutions, the actual 2:1 ratio between currents reduced after exertion of DMHT block from the trans- and the cis-side remains the same.

Perfusion of 100 mM KCl at the side of DMHT addition completely restored the α-LT-induced conductance after measurements had been made in the solutions with DMHT from either side of the BLM. Application of $CdCl_2$ (5 mM) onto a α-LT-induced current in 100 mM KCl solution from the side of DMHT addition further decreased K^+-current by 85±5% after the DMHT inhibition had fully developed from the cis- or the trans-side of the lipid bilayer. This coincides with the intensity of Cd^{2+} block in 100 mM KCl solution without DMHT (Fig. 6A inset).

3.2.5. The effect of TBA

Application of TBA (5 mM), known as a blocker of the ion channels with a pore diameter of 1.1 nm [13] from the cis-side of membrane decreased the α-LT-induced K^+-current only by 12±2% (Fig. 6A). The steady-state I/V plots of inwardly elicited K^+-current via α-LT channels also revealed small decrease in current after the cis-addition of this blocker (Fig. 6A, curve 3). This may suggest that the effective radius of α-LT channel on the cis-side is much larger then hydrodynamic radius of TBA molecule.

3.3. The influence of DMHT on RTX and α-LIT channels

Application of DMHT (0.1 mM) to the cis-side in 100 mM KCl solution inhibited the inward transmembrane current through the RTX channels by 50±5% within 1–2 min (Fig. 6B). Introduction of DMHT to the cis-side in 10 mM $CaCl_2$ solution also led to 2-fold decrease of initial conductance measured for RTX channels before the addition of inhibitor (data not shown). The ion substitution in this case might be ineffective because of weak monovalent cation selectivity and no selectivity to divalent cations found for RTX channels in BLM [12], while α-LT and α-LIT channels in bilayer membrane were proven to be ideally selective to monovalent cations and weakly Ca^{2+}-selective within the range of other physiologically significant divalent cations [6,18]. This suggestion could be confirmed by the fact that addition of DMHT (0.1 mM) on the cis-side of BLM reduced α-LIT conductance by 52±4% in the solution of 10 mM $CaCl_2$ and

Table 1
The α-LT and α-LIT single channel conductances and fillings with different nonelectrolytes

Nonelectrolyte	g_{both} of α-LT, pS	g_{trans} of α-LT, pS	F_{both} of α-LT	F_{trans} of α-LT	g_{both} of α-LIT, pS	F_{both} of α-LIT
1. –	165	–	–	–	23.5±4.8	–
2. Ethylene glycol	95	131	1.54	0.31	15±4.9	1.18
3. Glycerol	95	170	1.54	−0.06	15±4.6	1.18
4. Glucose	95	170	1.54	−0.06	15±4.4	1.18
5. Sucrose	95	170	1.54	−0.06	22±3.8	0.142
6. PEG 300	95	170	0.99	−0.04	24±5.2	−0.028
7. PEG 400	115	170	0.59	−0.04	24±3.6	−0.028
8. PEG 600	120	–	0.51	–	24±4.2	−0.028
9. PEG 1000	170	170	−0.04	−0.04	24±3.8	−0.028
10. PEG 1500	170		−0.04		24±3.8	−0.028
11. PEG 2000	170		−0.04		25±4.0	−0.081
12. PEG 3000	170		−0.04		25±4.4	−0.081
13. PEG 4000	170		−0.04		25±5.3	−0.081
14. PEG 6000	180		−0.11		25±5.2	−0.081
15. PEG 20000	180		−0.11			

All the NEs were used at a concentration of 20% in the membrane bathing fluid containing 100 mM KCl and 10 mM Tris–HCl (pH 7.4). The α-LT single channel conductance was defined from the peak of the amplitude histogram (Fig. 1) obtained on more then 100 separate channels. The α-LIT single channel conductance represents the mean value±standard errors obtained from more then 100 unitary channel conductances (Fig. 2). g_{both} refers to the single channel conductance determined in the presence of the same NE on both sides of the bilayer membrane and g_{trans} represents the single channel conductance measured in the presence of the required NE on the trans-side of the membrane, while PEG 1000 was placed at the cis-side. F_{both} is the ion channel filling with the same NE on both sides of a bilayer membrane. F_{trans} is the ion channel filling with the required NE on the trans-side of the membrane, while PEG 1000 was placed at the cis-side.

only by 25±3% in the solution of 100 mM KCl (Fig. 7). The DMHT inhibitory action had fully developed within 1–2 min time frame (Fig. 7A). The I/V curves plotted at positive potentials also exhibited decrease in conductance (Fig. 7B). The DMHT inhibition of α-LIT and RTX channels was fully reversible. Flushing cis-compartment with membrane bathing solution that did not contain DMHT restored the conductance of α-LIT and RTX channels measured before the addition of inhibitor.

3.4. Pore size determination

3.4.1. Traversing RTX pore

Addition of TBA (5 mM) to the cis-side of the BLM resulted in 90±3% blocking of transmembrane current through the RTX channels in 100 mM KCl solution (Fig. 6B). The I/V relationships of RTX channels also revealed a large conductance fall at positive potentials (Fig. 6B, curve 3). The TBA

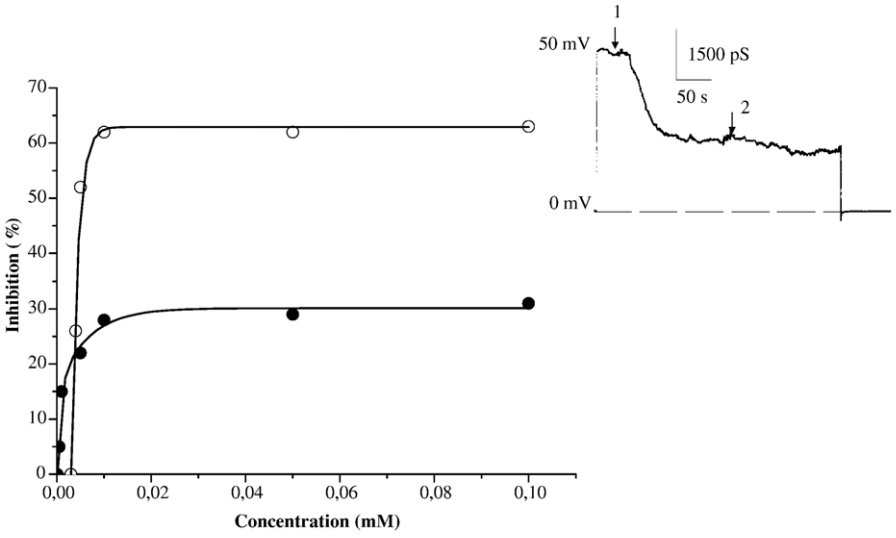

Fig. 4. The α-LT-induced conductance against DMHT concentrations applied from the different sides of the membrane. The BLM bathing fluid consisted of 10 mM $CaCl_2$ and the indicated DMHT concentrations. White circles (○) represent the consecutive DMHT additions made on the trans-side of the BLM. Black circles (●) represent the consecutive additions of DMHT made on the cis-side of the BLM. Cis- and trans-applications of DMHT were curried out separately on different membranes. The plots are best exponential fits to the experimental points. The membrane conductance was continuously monitored at 50 mV voltage clamp conditions. The inhibition percentages indicated are those achieved at the steady state. The α-LT was added to the cis-side of the BLM at a final concentration of 0.01 ng/ml. The inset is a dose-response time-trace of α-LT-induced current obtained after addition of saturating DMHT concentrations to the trans-chamber. Arrow 1 represents the introduction of 5 μM DMHT. Arrow 2 represents the consecutive addition of DMHT to the final concentration of 10 μM in the chamber. Dashed line indicates zero current.

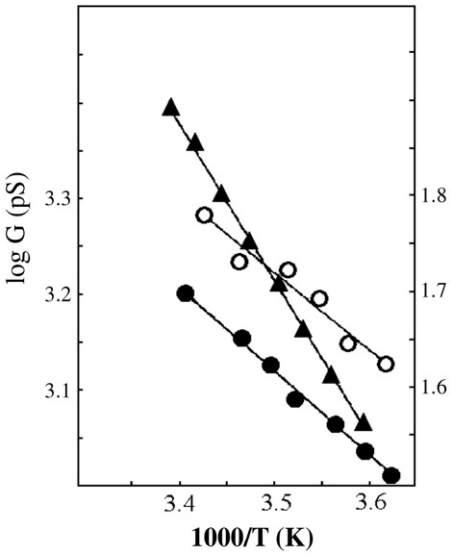

Fig. 5. The temperature relationships of α-LT-induced conductance of the bilayer lipid membrane. The membrane washing solution contained 10 mM $CaCl_2$. The conductance was continuously monitored at a membrane potential of +50 mV. α-LT was applied to the cis-side of the membrane at a final concentration of 0.01 ng/ml. (○)—Control experiments without DMHT or Cd^{2+} (left), (●)—DMHT (0.1 mM) was added from the cis-side of membrane (left), (▲)—$CdCl_2$ (1 mM) was added on the cis-side of the membrane (right). Each point represents average data of 8–10 experiments carried out on a separate membrane. Deviations of mean values had the same size with experimental points.

block of RTX channels conductance was reversible. Careful washout with 80 ml of KCl solution completely restored the conductance of RTX channels measured before the addition of blocker.

3.4.2. The effects of NEs on potassium current through α-LT channels

The radii of toxin pores from the cis- and trans-side of bilayer membrane were defined by the method based on the determination of channel filling with different NE molecules through each entrance of the channel [17]. Addition of NEs with various hydrodynamic radii to a 100 mM KCl membrane bathing solution alters the ionic current passing across the channel. Introduction of small well permeant NEs from both sides of BLM filled the channel lumen that resulted in decrease in potassium current via the channel. The single channel conductance increases as the hydrodynamic radius of NE approaches the effective radius of channel pore. The change of transmembrane potassium current was not sufficient in solutions containing NE molecules with hydrodynamic radii exceeding the size of channel pore (Table 1, Figs. 1c, d, 2c, d). The first NE within the range of NEs with different molecular weights (Table 1) that produced no effect on single channel conductance in the solution of potassium chloride was considered the closest to the size of channel lumen. The measurements of single channel conductance in symmetric solution of KCl with the same NEs on both sides of bilayer membrane provided a novel approach for separate pore size determination from the cis-side.

The most probable unitary conductance of α-LT channels in a solution of 100 mM KCl was 165 pS (Table 1, Fig. 1a). PEG 1000 became the first NE that did not decrease the conductance of α-LT, when placed from both sides of membrane (Table 1, Fig. 1c). Assuming that the effective radius of the ion channel on the cis-side is close to the minimal size of an impermeable NE molecule, the radius of the α-LT pore was determined within the transition zone from limited permeation of PEG 600 to impermeability at zero NE filling of the channel cavity (F_{both}, %=0). Thus, the radius of α-LT cis-entrance was 0.9±0.05 nm (Fig. 8). The percentage of the channel filling with the same NE on both sides of membrane (F_{both}, %) was defined as

$$2F_{both}/(F_1 + F_2) \times 100\%, \quad (1)$$

where F_{both} is the filling in the presence of a given NE, and F_1 and F_2 are the fillings in the presence of ethylene glycol and glycerol in membrane bathing solutions, correspondingly. The dependence of F_{both}, % on the hydrodynamic radii of NEs is represented in Fig. 8. The NE channel filling at symmetrical conditions (F_{both}) was calculated as

$$[g_0 - g_{both}/g_{both}]/[(k_0 - k_{20\%})/k_{20\%}], \quad (2)$$

where g_0 is the single channel conductance in a solution of 100 mM KCl, g_{both} is the single channel conductance in symmetric 20% water–salt solutions with different NEs, and $k_{20\%}$ and k_0 are the conductivities of 100 mM KCl solution with and without 20% NE, respectively [17,19].

To determine the filling of α-LT channel from the trans-entrance, a solution containing first impermeant NE (PEG 1000) was placed at the cis-side of membrane, whereas the trans-side of the membrane contained test NEs within the range of hydrodynamic radii applied for pore size determination (Table 1). Flushing 20 ml of required NE solution from the trans-side of BLM completely substituted initial symmetric solution containing PEG 1000 on both sides of membrane. The most probable unitary conductance of α-LT channel in the symmetric potassium chloride solution with PEG 1000 on both sides of membrane did not exceed the conductance of α-LT channels (g_{trans}, see Table 1) found in the solution containing PEG 1000 from the cis-side and glycerol from the trans-side of BLM (170 pS) (Table 1, Fig. 1e, trace 3). Moreover, g_{trans} of α-LT channel in a symmetrical potassium chloride solution with PEG 1000 from the cis-side and glucose, sucrose (Table 1, Fig. 1e, traces 2,1), PEG 300, PEG 400 from the trans-side of membrane was also 170 pS. Looking through the data represented in Table 1 one can see that g_{trans} of α-LT channel is larger then g_{both} within the range of NE molecules with hydrodynamic radii from 0.308 nm of glycerol up to 0.68 nm of PEG 400. The differences observed between the values of g_{both} and g_{trans} suggest the smaller size of the trans-entrance, since impermeable NEs on the trans-side let more K^+-current through the channel, thereby increasing its conductance. g_{trans} is larger then g_{both} when glycerol is from the trans-side and remains constant for the rest of NEs tested on the trans-side, besides ethylene glycol. Assuming that impermeable NEs almost do not change channel

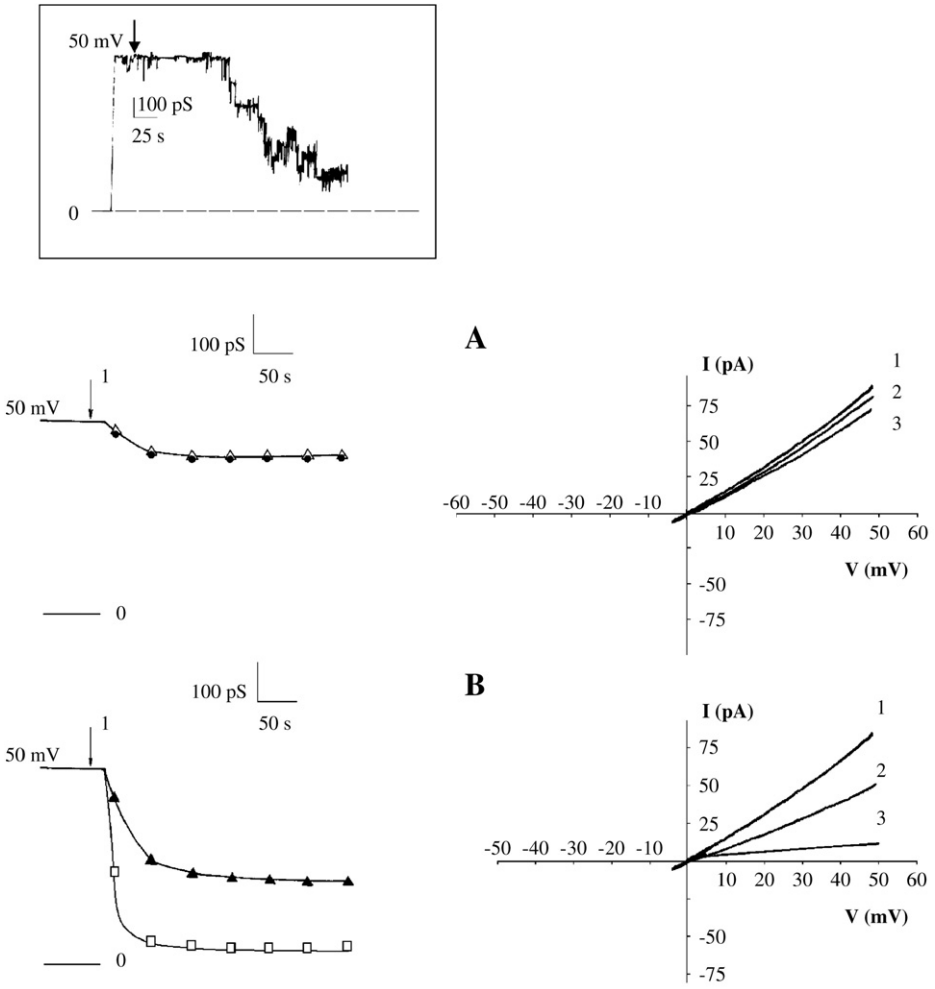

Fig. 6. Blocking of α-LT and RTX channels by TBA (5 mM) and DMHT (0.1 mM). The membrane was bathed in a symmetric solution of 100 mM KCl. A holding potential was +50 mV. In all the experiments, toxins were applied to the cis-side of the membrane at a concentration of 0.01 ng/ml. (A) (left) The time-courses of transmembrane current via α-LT channels after addition of (●)—TBA or (Δ)—DMHT to the cis-side. The inset is the time-trace of α-LT-induced current at +50 mV in a symmetric solution of 100 mM KCl after addition of $CdCl_2$ (5 mM) to the cis-side of membrane. The arrow indicates addition of Cd^{2+}. Dashed line shows zero current. (right) I/V relationships of the bilayer lipid membrane modified with α-LT in a symmetric solution of 100 mM KCl (plot 1), after cis-addition of DMHT (plot 2) and TBA (plot 3). (B) (left) The time-courses of transmembrane current through RTX channels after the addition of DMHT (▲) or TBA (□) to the cis-side of the membrane. (right) The I/V relationships of the bilayer lipid membrane modified by RTX in a symmetric solution of 100 mM KCl (plot 1) and after cis-addition of DMHT (plot 2) or TBA (plot 3). Each point of the left panels represents an average result of 8–10 experiments carried out on a separate membrane. Standard deviations did not exceed the size of experimental points. The sequential application of blockers represented on the panels from the right side was made after careful washout of the cis-compartment from the solution containing previously added blocker. The data obtained after the consecutive addition of blockers made on one membrane were the same with the results on separate addition (each made on a new membrane). Each right panel represents a different membrane. Arrows (1) indicate introduction of TBA or DMHT. Current–voltage relationships were determined using the voltage ramp protocol (−5 mV to +50 mV, 55 s).

conductance, it is possible that the trans-entrance of α-LT channel has the radius that does not exceed the size of a glycerol molecule.

In support of this suggestion, the g_{trans} of α-LT for all test NEs is also larger then the conductance of α-LT channel in the NE free symmetric solution of 100 mM KCl that can only happen if these NEs do not permeate through the channel on the trans-side because impermeable NEs are capable to increase the K^+ mobility in the basic solution of 100 mM KCl. The increased mobility of K^+ in the solutions containing impermeable NEs results in larger concentration of potassium ions inside the channel cavity compared with the regular amount of K^+ within the channel in symmetric solution of NE free 100 mM KCl [17,19]. This leads to the increase in α-LT single channel conductance (g_{trans}) in NE-salt solutions (glycerol, glucose, sucrose, PEG 300, PEG 400 and PEG 1000 on the trans-side vs. PEG 1000 on the cis-side) over the α-LT single channel conductance measured in symmetric 100 mM KCl (170 pS for all test NEs and 165 pS, correspondingly) and salt solutions containing permeable NEs (g_{both} from ethylene glycol to PEG 600).

The 23% conductance fall within the range of g_{trans} measured for α-LT channels occurred only when ethylene glycol was placed from the trans-side against PEG 1000 from the cis-side (Table 1, Fig. 1e, trace 4). The most probable α-LT single channel conductance dropped to 131 pS as compared with 170 pS for the rest of test NEs. Thus, the ethylene glycol is the first permeable NE of all tested on the trans-side. Assuming that the

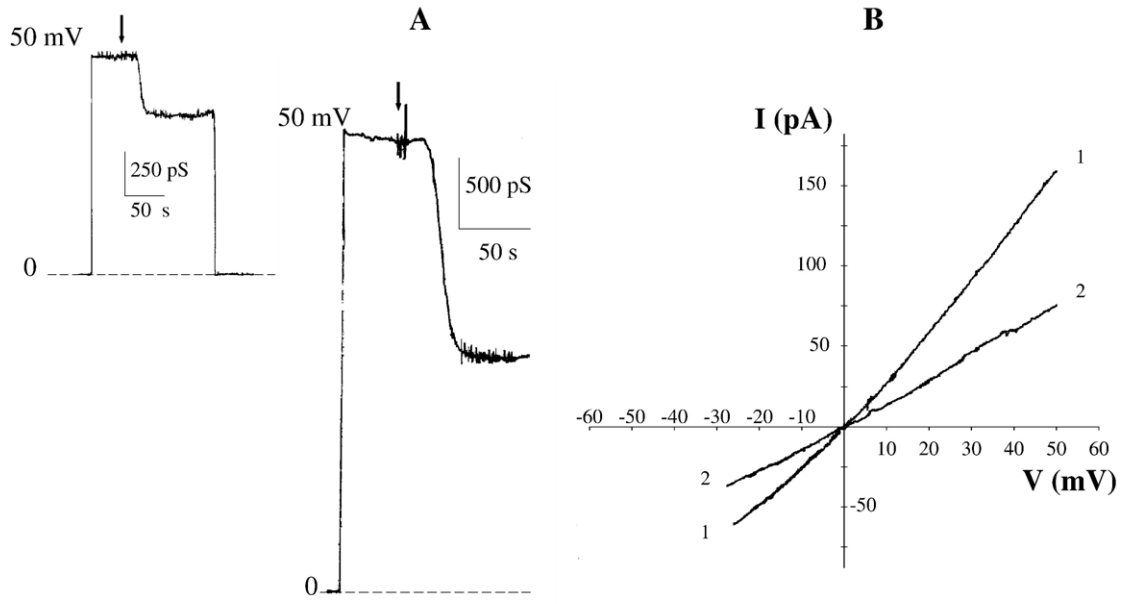

Fig. 7. DMHT (0.1 mM) inhibiting of the steady-state Ca^{2+} and K^+ currents across α-LIT channels. (A) The time-trace of α-LIT-induced current after addition of DMHT to the cis-side of membrane washed in the symmetric solution of 10 mM $CaCl_2$. Inset represents the time-trace of current through α-LIT channels after addition of DMHT to the cis-side of the membrane washed in the symmetric solution of 100 mM KCl. The membrane potential was +50 mV. The arrows indicate addition of DMHT. Each time-trace was recorded on a separate membrane. Dashed lines indicate zero current. (B) Current–voltage relationships of α-LIT channels were determined using the voltage ramp protocol (−30 mV to +50 mV, 1.3 min) in a symmetric solution of 10 mM $CaCl_2$ (plot 1) and after the addition of DMHT to the cis-side of the membrane (plot 2). In all the experiments α-LIT was introduced to the cis-side of the membrane at a final concentration of 0.043 ng/ml.

effective radius of the α-LT channel is supposed to be close to the minimal size of the first impermeable NE molecule after permeable ethylene glycol, we suggest that the apparent radius of α-LT pore trans-entrance is about the size of glycerol molecule in water–salt solution (0.308 nm). The mean value of the effective radius for α-LT trans-entrance has to be within the transition zone from limited permeation of ethylene glycol to impermeability at no NE filling of the channel cavity. Taking into account that the difference between hydrodynamic radii of glycerol and ethylene glycol is below the lowest standard deviation of the method (0.046 nm and 0.05 nm, correspondingly) [19], we propose to consider the mean value for the radius of α-LT trans-entrance as an arithmetic average of glycerol and ethylene glycol hydrodynamic radii (0.28± 0.18 nm).

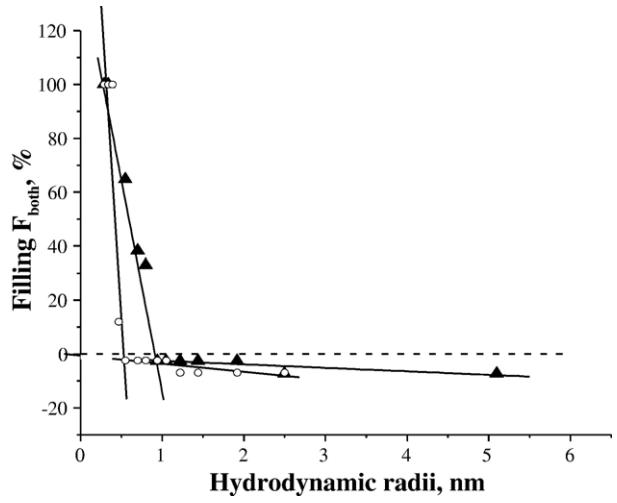

Fig. 8. The dependence of α-LT and α-LIT single channel filling from both entrances (F_{both}, %) on the hydrodynamic radii of nonelectrolytes. The conductances of α-LT (▲) and α-LIT (○) channels, represented in Table 1, were defined in solutions of the same NEs from both sides of the membrane. F_{both}% of α-LT is not shown for sucrose and glucose. Dashed line indicates zero filling of α-LT and α-LIT channels with NE molecules. All other lines are best least square fits to the experimental points. Standard deviations of each mean value represented in Table 1. Additional information on experimental conditions described in the legends to Fig. 1, Fig. 2 and Table 1.

3.4.3. Determination of the α-LIT pore size on the cis-side of a bilayer membrane

The average unitary conductance of α-LIT channel in a solution of 100 mM KCl was 23.5 pS (Table 1, Fig. 2a). Sucrose became the first NE that did not produce a considerable reduction of this conductance after symmetrical introduction from the both sides of BLM. Estimates of the α-LIT pore size made within the transition zone from limited permeation of sucrose to impermeability at zero NE filling of the channel suggested that the radius of α-LIT cis-entrance was 0.53± 0.05 nm (Fig. 8).

4. Discussion

DMHT has been proven to be one of the most efficient thiazole derivatives, which depresses spontaneous and α-LT evoked acetylcholine release and neuromuscular transmission

due to its presynaptic action. Application of DMHT at low concentration (100 μM) almost completely eliminated the α-LT-induced increase in the frequency of miniature end-plate potentials (MEPPs) in cholinergic synapses of the vertebrate skeletal muscles [1,2]. Until now a molecular mechanism for the interaction of DMHT with excitable membranes or α-LT had not been demonstrated, although on the basis of structural similarities of thiamine thiazole analogues it was suggested that the thiazole moiety of DMHT molecules may bind with thiamine-sensitive membrane sites [1]. The direct interaction with endogenous channels or α-LT also seems possible, since α-LT and other toxins, relatively recently isolated from black widow spider venom, have been found to form channels in artificial and native membranes [4,6,11,12,18,20]. Application of lipid bilayer technique has provided a convenient tool for investigation of pore-forming toxins. It seemed valuable, therefore, to reconstitute α-LT, α-LIT and RTX channels in order to ascertain their interaction with DMHT. The data presented in this work clearly show that DMHT readily inhibits transmembrane currents of physiologically significant cations (Ca^{2+} and K^{+}) through α-LT channels. Although the depression of transmembrane current occurred on both sides of the membrane, DMHT blocked two times more current after addition to the trans-chamber. This leads to believe that the channel's DMHT binding site is better accessible from the trans-side of BLM. It is also possible that DMHT exerts its inhibiting action due to penetration into the channel cavity. Therefore, the asymmetric action of DMHT on α-LT channel (Fig. 3) may result from the different diameters of the channel on the opposite sides of the membrane as suggested earlier on the basis of cryo-electron microscopy data [8]. In case, the binding of DMHT to α-LT occurs within the channel pore, the possibility of DMHT partitioning into membrane hydrophobic phase appears to be not of importance for the mechanism.

The coincidence of Cd^{2+} blocking effect after DMHT-induced inhibition of Ca^{2+}-current with the intensity of Cd^{2+} block in control experiments without DMHT, found from both sides of α-LT channel, suggests no considerable influence of DMHT molecule on Ca^{2+}-binding side inside the toxin pore. This could be confirmed by complete reversibility of DMHT inhibition of α-LT and other toxin channels after washout and no significant change of E_a for Ca^{2+}-current through α-LT channels after interacting with DMHT (8.501±0.879 kJ/mol in 10 mM $CaCl_2$ and 9.255±0.126 kJ/mol after DMHT-induced inhibition) compared with Cd^{2+} (12.102±0.419 kJ/mol after Cd^{2+}-block had developed) (Fig. 5).

The binding kinetics of DMHT with the α-LT channel shows no cooperativity and allows to expect that the toxin's binding site is formed by only one charged group as the slopes of inhibition rate determined in log–log coordinates are 1.25 on the trans-side and 0.68 on the cis-side. Similar pK of binding (5.4 on the trans-side and 5.7 on the cis-side) also suggest the involvement of the same DMHT binding site of α-LT channel that could be accessible for the inhibitor from either side of the BLM.

Estimates of the α-LT pore size made from the cis- and the trans-side of BLM using different NEs to fill the channel lumen suggested that the effective radius of α-LT cis-entrance was three times larger then that of the trans-entrance (0.9±0.05 nm and 0.28±0.18 nm, respectively) (Table 1, Fig. 8). These data are in a good agreement with the structure of α-LT pore determined using cryo-electron microscopy, where the channel inside the membrane bound α-LT tetramer was 2.5 times wider from one side compared with another [8].

Taking into account the oriented insertion of α-LT into a lipid bilayer [11,18] and the most effective DMHT action on the trans-entrance of α-LT channel, it could be anticipated that the DMHT-induced reduction of MEPPs evoked by α-LT on excitable membrane [1,2] resulted from application of DMHT to a narrower portion of the channel.

With 7-fold difference between the conductances of relatively large α-LT and small α-LIT channels (165 pS and 23.5 pS, respectively), one can expect a smaller size for α-LIT pore. In support of this suggestion, the radius of the cis-entrance determined for α-LIT pore in the symmetrical NE solutions was 0.53±0.05 nm (Figs. 2, 8).

Addition of DMHT to the cis-side of α-LIT channel resulted in 52±4% inhibition of calcium current (Fig. 7). It seems likely, that DMHT inhibition was smaller on α-LT cis-entrance compared with α-LIT cis-entrance (31.6±3% and 52±4%, respectively) because of larger radius of α-LT pore (0.9±0.05 nm). On the contrary, a smaller radius of α-LT trans-entrance (0.28±0.18 nm) compared with α-LIT cis-entrance (0.53±0.05 nm) may have become a reason for larger DMHT inhibition from the trans-side of α-LT channel in calcium chloride solution (61.8±3%).

The TBA block of RTX pore from the cis-side indicates that the radius of its cis-entrance is almost the same with the molecular radius of the blocker (0.55 nm). With similar radii of the RTX and α-LIT cis-entrances (0.55 nm and 0.53 nm, correspondingly) it was possible to expect the same DMHT inhibiting. Indeed, the addition of DMHT from the cis-side of the membrane resulted in 50±5% block for RTX channels and 52±4% for α-LIT channels in the bathing solution of calcium chloride (Figs. 6, 7). One-side addition of TBA to the wider cis-entrance of α-LT channel (0.9±0.05 nm) inhibited only 12±2% of transmembrane current in potassium chloride solution, whilst it reduced 90±3% of current through narrower RTX channel (0.55 nm) (Fig. 6A, B).

Thus, the potency of DMHT and TBA inhibition increased on the smaller size channel lumens.

The inhibitory effects of DMHT and TBA found for pore-forming proteins that belong to different families of animal and plant toxins suggest that the specific interaction between these proteins and blockers, if any, is insignificant.

Though the indications that the exocytosis in nerve tissues can be promoted by alternative mechanisms [21,22], there is strong evidence that α-LT and α-LIT form ion-conductive pores in the excitable membranes, thereby provoking processes inside the nerve endings that finally lead to quantum neurotransmitter release [4,5,6,18]. Hence, the DMHT depression of α-LT-neurotransmitter release in nerve tissues of vertebrates may result from a direct inhibition of Ca^{2+} influx through α-LT pores in presynaptic membranes [23]. It also seems likely that α-LIT-

induced release of neurotransmitters that occurs in invertebrates [5] can be decreased by application of DMHT onto the α-LIT channel pores.

Acknowledgements

The authors wish to thank Drs M.F. Shuba of Bogomolets Institute of Physiology, Ukrainian National Academy of Sciences, Kiev, and S.A. Kosterin of Palladin Institute of Biochemistry, Ukrainian National Academy of Sciences, Kiev, for valuable comments, discussions and criticism. We are also indebted to Dr. Yu. M. Krasnopolsky of Kharkov Factory of Biopreparations, Joint-Stock Company "Biolek", Kharkov, for providing the cholesterol.

The temperature ramp was designed and built by Dr. S.V. Khlebnikov of National Technical University "Kiev Politechnical Institute". Special thanks to Dr. T.A. Borisova of Palladin Institute of Biochemistry, Ukrainian National Academy of Sciences, Kiev, Drs. M.V. Kustov, V.S. Telezhkin and V.V. Tsvilovsky of Bogomolets Institute of Physiology, Ukrainian National Academy of Sciences, Kiev, for friendly advice and support.

References

[1] A.V. Romanenko, A.I. Vovk, O.Ya. Shatursky, Effects of thiazole analogues of vitamin B_1 on neuromuscular transmission and α-latrotoxin-induced transmitter release in skeletal muscles, Neurophysiologia 27 (1995) 291–296.

[2] A.V. Romanenko, V.M. Gnatenko, I.A. Vladimirova, A.I. Vovk, Pre- and post-synaptic modulation of neuromuscular transmission in smooth muscles by thiazole analogs of vitamin B_1, Neurophysiologia 27 (1995) 297–306.

[3] A.I. Vovk, A.V. Romanenko, Thiazole analogs of vitamin B1 that depress neuromuscular transmission, Dokl. Acad. Nauk Ukr. 5 (1993) 119–121 (in Russian).

[4] A.K. Filippov, S.M. Tertishnikova, A.E. Alekseev, G.P. Tsurupa, V.N. Pashkov, E.V. Grishin, Mechanism of α-latrotoxin action as revealed by patch-clamp experiments on *Xenopus oocytes* injected with rat brain messenger RNA, Neuroscience 61 (1994) 179–189.

[5] L.G. Magazannik, I.M. Fedorova, G.I. Kovalevskaya, V.N. Pashkov, O.V. Bulgakov, E.V. Grishin, Selective presynaptic insectotoxin (α-latroinsectotoxin) isolated from black widow spider venom, Neuroscience 46 (1992) 181–188.

[6] O.Ya. Shatursky, V.N. Pashkov, O.V. Bulgacov, E.V. Grishin, Interaction of α-latroinsectotoxin from *Latrodectus mactans* venom with bilayer lipid membranes, Biochim. Biophys. Acta 1233 (1995) 14–20.

[7] K.E. Volynski, E.D. Nosyreva, Yu.A. Ushkaryov, E.V. Grishin, Functional expression of α-latrotoxin in baculuvirus system, FEBS Lett. 442 (1999) 25–28.

[8] E.V. Orlova, M.A. Rahman, B. Gowen, K.E. Volynski, A.C. Ashton, C. Manser, M. van Heel, Yu.A. Ushkaryov, Structure of α-latrotoxin oligomers reveals that divalent cation-dependent tetramers form membrane pores, Nat. Struct. Biol. 7 (2000) 48–53.

[9] A.W. Henkel, S. Sankaranarayanan, Mechanism of α-latrotoxin action, Cell Tissue Res. 296 (1999) 229–233.

[10] N. Kiyatkin, I. Dulubova, E. Grishin, Cloning and structural analysis of α-latroinsectotoxin cDNA. Abundance of ankyrin-like repeats, Eur. J. Biochem. 213 (1993) 121–127.

[11] I.E. Dulubova, V.G. Krasnoperov, M.V. Khvotchev, K.A. Pluzhnikov, T.M. Volkova, E.V. Grishin, H. Vais, D.R. Bell, P.N.R. Usherwood, Cloning and structure of δ-latroinsectotoxin, a novel insect-specific member of the latrotoxin family, J. Biol. Chem. 271 (1996) 7535–7543.

[12] A.N. Chanturia, O.Ya. Shatursky, V.K. Lishko, M.M. Monastyrnaya, E. P. Kozlovskaya, Sea anemone toxin (*Radianthus macrodactilus*) interaction with bilayer lipid membranes, Biol. Membr. 7 (1990) 763–769 (in Russian).

[13] V.L. Shnyrov, M.M. Monastyrnaya, G.G. Zhadan, S.M. Kuznetsova, E.P. Kozlovskaya, Calorimetric study of interaction of toxin from sea anemone *Radianthus macrodactylus* with erythrocyte membrane, Biochem. Int. 26 (1992) 219–229.

[14] O.Ya. Shatursky, A.V. Romanenko, The effect of a vitamin B1 thiazole analogue on ion channels formed by alpha-latrotoxin and sea anemone toxin in bilayer lipid membranes, Dokl. Biochem. Biophys. 384 (2002) 159–162 (in Russian).

[15] A.N. Chanturia, A.N. Nikolaenko, O.Ya Shatursky, V.K. Lishko, Probing the structure–function relationship of α-latrotoxin formed channels with antibodies and pronase, Toxicon 34 (1996) 1157–1164.

[16] R.O. Blaustein, A. Finkelstein, Voltage-dependent block of anthrax toxin channels in plane phospholipids bilayer membranes by symmetric tetraalkylammonium ions. Effects on macroscopic conductance, J. Gen. Physiol. 96 (1990) 905–919.

[17] O.V. Krasilnikov, J.B. DaCruz, L.N. Yuldasheva, W.A. Varanda, R.A. Nogueira, A novel approach to study the geometry of the water lumen of ion channels: Colicin Ia channels in planar lipid bilayers, J. Membr. Biol. 161 (1998) 83–92.

[18] S.L. Mironov, Yu.V. Sokolov, A.N. Chanturia, V.K. Lishko, Channels produced by spider venoms in bilayer lipid membrane: mechanisms of ion transport and toxic action, Biochim. Biophys. Acta 862 (1986) 185–198.

[19] R.Z. Sabirov, O.V. Krasilnikov, V.I. Ternovsky, P.G. Merzliak, Relation between ionic channel conductance and conductivity of media containing different nonelectrolytes. A novel method of pore size determination, Gen. Physiol. Biophys. 12 (1993) 95–111.

[20] O.Ya. Shatursky, T.M. Volkova, E.V. Grishin, Interaction of δ-latroinsectotoxin from black widow spider venom with the planar phospholipid membrane, Biol. Membr. 21 (2004) 333–342 (in Russian).

[21] L.G. Storchak, V.N. Pashkov, N.G. Pozdnyakova, N.G. Himmelreich, E.V. Grishin, δ-latrotoxin-stimulated GABA release can occur in $Ca2^+$-free medium, FEBS Lett. 351 (1994) 267–270.

[22] L.G. Storchak, M.V. Linetska, N.G. Himmelreich, Does extracellular calcium determine what pool of GABA is the target for α-latrotoxin? Neurochim. Int. 40 (2002) 387–395.

[23] A.C. Ashton, M.A. Rahman, K.E. Volynski, C. Manser, E.V. Orlova, H. Matsushita, B.A. Davletov, M. van Heel, E.V. Grishin, Yu.A. Ushkaryov, Tetramerization of α-latrotoxin by divalent cations is responsible for toxin-induced non-vesicular release and contributes to the $Ca2^+$-dependent vesicular exocytosis from synaptosomes, Biochimie 82 (2002) 453–468.